

# UCSF

## UC San Francisco Previously Published Works

### Title

Induced Pluripotent Stem Cell Models of Progranulin-Deficient Frontotemporal Dementia Uncover Specific Reversible Neuronal Defects

### Permalink

<https://escholarship.org/uc/item/2rw5x4fb>

### Journal

Cell Reports, 2(4)

### ISSN

2639-1856

### Authors

Almeida, Sandra

Zhang, Zhijun

Coppola, Giovanni

et al.

### Publication Date

2012-10-01

### DOI

10.1016/j.celrep.2012.09.007

### Copyright Information

This work is made available under the terms of a Creative Commons Attribution License, available at <https://creativecommons.org/licenses/by/4.0/>

Peer reviewed



Published in final edited form as:

Cell Rep. 2012 October 25; 2(4): 789–798. doi:10.1016/j.celrep.2012.09.007.

## Induced Pluripotent Stem Cell Models of Progranulin-Deficient Frontotemporal Dementia Uncover Specific Reversible Neuronal Defects

Sandra Almeida<sup>1</sup>, Zhijun Zhang<sup>1</sup>, Giovanni Coppola<sup>2,7</sup>, Wenjie Mao<sup>3</sup>, Kensuke Futai<sup>3</sup>, Anna Karydas<sup>4</sup>, Michael D. Geschwind<sup>4</sup>, M. Carmela Tartaglia<sup>4,8</sup>, Fuying Gao<sup>2</sup>, Davide Gianni<sup>1</sup>, Miguel Sena-Esteves<sup>1</sup>, Daniel H. Geschwind<sup>2</sup>, Bruce L. Miller<sup>3</sup>, Robert V. Farese Jr.<sup>5,6</sup>, and Fen-Biao Gao<sup>1,\*</sup>

<sup>1</sup>Department of Neurology, University of Massachusetts Medical School, Worcester, MA 01605, USA

<sup>2</sup>Department of Neurology, David Geffen School of Medicine, University of California, Los Angeles, CA 90095, USA

<sup>3</sup>Brudnick Neuropsychiatric Research Institute, Department of Psychiatry, University of Massachusetts Medical School, Worcester, MA 01605, USA

<sup>4</sup>Memory and Aging Center, Department of Neurology, University of California, San Francisco, CA 94143, USA

<sup>5</sup>Gladstone Institute of Cardiovascular Disease, San Francisco, CA 94158, USA

<sup>6</sup>Departments of Medicine and Biochemistry and Biophysics, University of California, San Francisco, CA 94158, USA

### SUMMARY

The pathogenic mechanisms of frontotemporal dementia (FTD) remain poorly understood. Here we generated multiple induced pluripotent stem cell (iPSC) lines from a control subject, a patient with sporadic FTD, and an FTD patient with a novel *GRN* mutation (PGRN S116X). In neurons and microglia differentiated from PGRN S116X iPSCs, the levels of intracellular and secreted progranulin were reduced, establishing patient-specific cellular models of progranulin haploinsufficiency. Through a systematic screen of inducers of cellular stress, we found that PGRN S116X neurons, but not sporadic FTD neurons, exhibited increased sensitivity to staurosporine and other kinase inhibitors. Moreover, the serine/threonine kinase S6K2, a component of the PI3K and MAPK pathways, was specifically downregulated in PGRN S116X

© 2012 Elsevier Inc. All rights reserved.

\*Correspondence to Fen-Biao Gao, Department of Neurology, University of Massachusetts Medical School, Worcester, MA 01605. fen-biao.gao@umassmed.edu.

<sup>7</sup>Present address: Departments of Psychiatry & Neurology, David Geffen School of Medicine, University of California, Los Angeles, CA 90095, USA

<sup>8</sup>Present address: Krembil Neuroscience Centre and University of Toronto, Canada

**Publisher's Disclaimer:** This is a PDF file of an unedited manuscript that has been accepted for publication. As a service to our customers we are providing this early version of the manuscript. The manuscript will undergo copyediting, typesetting, and review of the resulting proof before it is published in its final citable form. Please note that during the production process errors may be discovered which could affect the content, and all legal disclaimers that apply to the journal pertain.

### ACCESSION NUMBERS

Microarray data are available at the NCBI Gene Expression Omnibus database under the series accession number GSE40378.

### SUPPLEMENTAL INFORMATION

Supplemental Information includes Extended Experimental Procedures, four figures, and one table.

neurons. Both increased sensitivity to kinase inhibitors and reduced S6K2 were rescued by progranulin expression. Our findings identify cell-autonomous, reversible defects in patient neurons with progranulin deficiency and provide a new model for studying progranulin-dependent pathogenic mechanisms and testing potential therapies.

## Keywords

frontotemporal dementia; haploinsufficiency; iPSCs; kinases; microglia; neurons; progranulin; stress; S6K2

## INTRODUCTION

Frontotemporal dementia (FTD), the second most common form of presenile dementia before the age of 65, is associated with focal atrophy of the frontal or temporal lobes and deficits in cognition, behavior, and language (Boxer and Miller, 2005). Mutations that cause FTD have been identified in several genes, including those encoding valosin-containing protein (Watts et al., 2004), charged multivesicular body protein 2B (Skibinski et al., 2005), progranulin (*GRN*) (Baker et al., 2006; Cruts et al., 2006), and chromosome 9 open reading frame 72 (DeJesus-Hernandez et al., 2011; Renton et al., 2011). It is not known how these diverse mutations cause similar clinical manifestations, and no effective treatment is available.

The secreted glycoprotein progranulin has been implicated in cell growth and survival, inflammation, synaptic functions, and other cellular functions (He and Bateman, 2003; Yin et al., 2010; Tapia et al., 2011). Although most if not all pathogenic mutations in *GRN* lead to pathological changes in FTD due to progranulin haploinsufficiency (Baker et al., 2006; Cruts et al., 2006), the underlying molecular mechanism is unknown. Progranulin mutations are a common cause of FTD. However, no robust pathological phenotype has been found in *Grn*<sup>+/-</sup> mice, and selective neuronal cell loss is limited even in *Grn* knockout mice (Ahmed et al., 2010; Ghoshal et al., 2012; Petkau et al., 2012; Yin et al., 2010). Thus, a more suitable model for dissecting the pathogenic mechanisms underlying progranulin haploinsufficiency is needed.

The ability to generate human induced pluripotent stem cells (iPSCs) offers an unprecedented opportunity to analyze the molecular consequences of pathogenic mutations in the context of the unique genetic background of individual patients (Yamanaka, 2007). Indeed, iPSCs have been generated from patients with different neurodegenerative diseases (e.g. Dimos et al., 2008; Ebert et al., 2009; Soldner et al., 2009; Nguyen et al., 2011; Israel et al., 2012). In this study, we generated multiple FTD patient-specific iPSC lines and established a human neuronal model of progranulin haploinsufficiency. From studies of human postmitotic neurons derived from these lines, we identify cell-autonomous and reversible defects in specific signaling pathways that are compromised in progranulin (PGRN)-deficient neurons.

## RESULTS

### Generation and Characterization of FTD Patient-Specific iPSCs

The two FTD patients under investigation in this study are part of a longitudinal dementia research program at the University of California, San Francisco (UCSF) Memory and Aging Center. Both had an 8-year history of behavioral changes and memory impairment at the time of tissue collection for this study. One patient, a 67-year-old male with sporadic FTD, tested negative for mutations in *GRN*, *MAPT*, and *C9ORF72*. The other patient, a 64-year-

old male with a significant family history, had behavioral variant frontotemporal dementia. Magnetic resonance imaging (MRI) in this patient demonstrated severe bifrontal and temporal atrophy associated with gliosis in the frontal lobes (greater on the right). One year later, MRI scans showed progression of atrophy and gliosis. Genetic testing revealed a novel nonsense mutation in *GRN*, p.S116X (g.4627C>A, c.347C>A), predicted to result in a premature stop codon. Both FTD patients had parkinsonism, which is typical in all FTD patients with progranulin mutations. An age-matched subject, a clinically normal 64-year-old male with no mutations in *GRN*, *MAPT*, or *C9ORF72*, served as a control.

Skin biopsies from the upper right thigh were obtained from all three subjects, and primary fibroblasts were derived. After expansion, the fibroblasts were reprogrammed with four transcription factors (OCT3/4, SOX2, KLF4, and CMYC) into putative pluripotent stem cells as described (Takahashi et al., 2007). Approximately 5 weeks after viral transduction, more than 50 iPSC colonies per subject were picked on the basis of their embryonic stem cell (ESC)-like morphology and expanded further on feeder cells.

To identify lines in which the exogenous reprogramming factors were completely silenced, we characterized 10-15 putative iPSC lines from each subject by quantitative RT-PCR (qRT-PCR). Complete transgene silencing was achieved when the total expression of each reprogramming factor was not different from that of the endogenous gene (Figure 1, A-C). This assay allows us to detect transgene expression levels at least up to 20 times the endogenous ESC H9 levels. Based on this analysis, three lines per subject were selected for further characterization: control lines 16, 17, and 20 (Figure 1A); sporadic FTD lines 9, 12, and 23 (Figure 1B); and PGRN S116X lines 1, 14, and 26 (Figure 1C). The total expression of each reprogramming factor was not different from that of the endogenous gene (Figure 1, A-C), indicating complete transgene silencing. All lines expressed marker genes of undifferentiated ESCs, such as *OCT3/4*, *SOX2*, and *NANOG*, at levels comparable to those in ESC line H9. Two additional stem cell markers, teratocarcinoma-derived growth factor 1 (TDGF1, or CRIPTO) and zinc finger protein 42 (ZFP42, or Rex1), were also expressed at levels equivalent to those in H9 cells (Figure S1A).

Sequencing confirmed that the PGRN S116X iPSC lines retained the *GRN* nonsense mutation (g.4627C>A, c.347C>A) (Figure 1D). Analysis of the *OCT4* promoter region showed that undifferentiated iPSCs were hypomethylated relative to the respective fibroblasts from which they were derived (Figure 1E). In addition, iPSCs expressed the stem cell-specific surface proteins SSEA4, TRA-1-60, TRA-1-81, NANOG, and OCT4, as shown by immunostaining (Figure 1F and Figure S1B). All nine iPSC lines maintained a normal karyotype after reprogramming (Figure 1F and Figure S1C) and could spontaneously differentiate into cell types of all three germ layers in vitro (Figure 1G and Figure S1C). Moreover, representative iPSC lines from the subjects (control line 20, sporadic line 9, and PGRN S116X line 26) transplanted into SCID mice gave rise to teratomas in vivo (Figure 1G). These findings confirm the successful reprogramming and generation of FTD patient-specific iPSC lines and demonstrate that these lines are similar to controls in both their expression of stem cell markers and their pluripotency.

### Differentiation of FTD-Patient Specific iPSCs into Neurons

Next, we differentiated three fully reprogrammed iPSC lines at passages 20-26 from each subject into postmitotic neurons, using a protocol available in our lab (Delaloy et al., 2010). The differentiation starts with neural induction, which is followed by expansion of the neural progenitor cells and neural maturation. The first step, induction of multilineage differentiation and embryoid body (EB) formation, was inefficient when iPSCs were maintained on feeder cells. Adaptation of iPSCs to feeder-free conditions allowed robust and reliable formation of EBs (Figure 2, A and B). After 5-6 days in suspension, neural

induction was initiated with basic fibroblast growth factor and N2 supplement, and rosettes—elongated cells arranged in circular structures—appeared (Figure 2C). Ten days later, rosettes were isolated, expanded in suspension as neurospheres for 3-4 weeks (Figure 2D), and dissociated into single cells. Terminal differentiation was induced with glial cell line-derived neurotrophic factor (GDNF), brain-derived neurotrophic factor (BDNF), ascorbic acid, and cyclic AMP. Two weeks later, the cells displayed typical neuronal morphology (Figure 2F). Both FTD and control iPSCs differentiated at similar rates.

Then we determined whether the disease and/or mutation affect the percentage of neurons obtained with this protocol. After 2 weeks, approximately 80% of cells in culture were positive for the neuronal marker microtubule-associated protein 2 (MAP2) and had neuronal morphology (Figure 2G), and less than 4% of cells were positive for the glial marker glial fibrillary acidic protein, regardless of the genetic mutation of the iPSC line used (Figure 2, G and K). Thus, the PGRN S116X mutation did not affect the percentage of neurons generated with the differentiation protocol. Approximately 40% of the MAP2<sup>+</sup> cells were presumably glutamatergic and expressed VGLUT1 (Figure 2H), and less than 10% of cells were GABA<sup>+</sup> inhibitory neurons or TH<sup>+</sup> dopaminergic neurons (Figure 2, I and J). Again, the percentages of neurons differentiated from control and FTD patient-specific iPSC lines were indistinguishable. Additional analysis at the mRNA level indicative of glutamatergic (*VGLUT1*), GABAergic (*GAD67*) and dopaminergic (*TH*) neuronal subtypes or postsynaptic density (*PSD95*) detected no significant differences across the different lines (Figure S2, A-D). Thus, the PGRN S116X mutation did not affect neural differentiation of iPSCs into specific type of neurons.

We next performed whole-cell voltage clamp recording, and measured membrane properties and synaptic transmission on neurons differentiated from two iPSC lines (control line 20 and PGRN S116X line 26) (Figure 2L-N). Most cells in culture were capable of inducing tetrodotoxin-sensitive action potentials (control: 79.2%, PGRN S116X: 75%), which is consistent with the finding that about 80% of cells are MAP2-positive neurons (Figure 2G). The resting membrane potential between two cell lines does not show a statistically significant difference (control neurons:  $-62.5 \pm 1.5$  mV, PGRN S116X:  $-60.0 \pm 1.9$  mV,  $n = 24$ ,  $p = 0.17$ ). To address whether these cells can form functional synaptic connections, we found that PSD95 puncta were present on dendrites of these neurons (Figure S2E) and also measured AMPA-type glutamate receptor-mediated miniature excitatory postsynaptic currents (mEPSCs). Neurons differentiated from PGRN S116X iPSCs showed synaptic connection indistinguishable from control neurons [mEPSC amplitude of control neurons:  $12.1 \pm 1.7$  pA, PGRN S116X:  $14.37 \pm 1.7$  pA,  $p = 0.36$ ; frequency of control neurons:  $3.2 \pm 0.6$  pA, PGRN S116X:  $2.2 \pm 0.2$  pA,  $n = 10$ ,  $p = 0.12$ ]. These results indicate that postmitotic neurons differentiated from control and PGRN S116X iPSCs are functional.

## A Human Neuronal Model of Progranulin Haploinsufficiency

To establish a human neuronal model of progranulin haploinsufficiency, we first examined the expression levels of progranulin in fibroblasts from each subject by qRT-PCR. *GRN* mRNA levels were similar in cells from the control subject and sporadic FTD patient (Figure 3A), but in cells from the FTD patient with the PGRN S116X mutation, the mRNA level was only about 30% of control (Figure 3A). This observation is consistent with the substantially lower average plasma progranulin levels in FTD patients harboring *GRN* mutations than in those without such mutations (Coppola et al., 2008; Finch et al., 2009). However, after reprogramming, the *GRN* mRNA was 50% lower in all three PGRN S116X iPSC lines (Figure 3B), as expected. Moreover, the relative expression levels of *GRN* mRNA in all control or sporadic FTD iPSCs showed little variation (Figure 3B). Correspondingly, PGRN S116X iPSCs secreted 50% less progranulin than iPSCs from the control subject and sporadic FTD patient (Figure 3C).

Upon differentiation, *GRN* mRNA levels were about 41% lower in PGRN S116X neurons than in control and sporadic FTD neurons differentiated from multiple iPSC lines (Figure 3D). The levels of both intracellular and secreted progranulin in these neurons were also correspondingly reduced, as measured by ELISA (Figure 3, E and F). Thus, we established a patient-specific human neuronal model of progranulin haploinsufficiency. We were also able to differentiate these iPSCs into microglia as shown by expression of the microglia-specific marker Iba1 (Figure S3, A and B). Progranulin secretion from these cells was also approximately 50% lower than in control and sporadic FTD cells (Figure S3, C and D).

### **PGRN S116X Neurons Are More Sensitive to Cellular Stress Induced by Inhibitors of the PI3K/Akt and MEK/MAPK signaling pathways**

Compared with many other neurodegenerative diseases, cellular defect associated with FTD remain poorly defined. Human neurons derived from patient-specific iPSCs are an excellent system to examine disease gene-specific cellular phenotypes. To this end, we first used two iPSC lines from each patient and differentiated them into postmitotic neurons. Under normal culture conditions, PGRN S116X and control neurons show similar viability. As a late-onset disease, FTD likely results from damage that accumulates over time rather than from an acute effect of the reduced progranulin levels. Very little is known about the cellular defects caused by progranulin haploinsufficiency in human neurons. Thus, to identify pathways that might be compromised in PGRN S116X neurons, we performed a systematic screen with a variety of inducers of cellular stress that affect different key cellular functions/pathways, such as mitochondria, oxidative stress, endoplasmic reticulum, proteasome, and cell survival. Neurons derived from the healthy individual and the sporadic FTD case were used as controls.

We tested two well-known inducers of mitochondrial dysfunction, oligomycin (an ATP synthase inhibitor) and rotenone (a complex I inhibitor), as well as a classical inducer of oxidative stress (hydrogen peroxide). All three inducers of cell stress reduced cell viability in dose-dependent manner, and all genotypes or disease states were equally affected (Figure S4, A, B; data on oligomycin not shown due to space limitations). In contrast, PGRN S116X neurons were more susceptible than control neurons to endoplasmic reticulum (ER) stress, induced by tunicamycin, an inhibitor of protein N-glycosylation (Figure 4A) and proteasome activity inhibition induced by lactacystin (Figure S4C). Because sporadic FTD neurons also showed similar enhanced sensitivity to tunicamycin and lactacystin (Figure 4A and Figure S4C), we concluded that these cellular phenotypes are not specific to progranulin deficiency.

To further explore progranulin-dependent cellular defects in FTD neurons, we also tested the effect of staurosporine, a broad-spectrum kinase inhibitor that induces apoptosis (Figure 4B). Interestingly, PGRN S116X neurons were more sensitive to staurosporine than control or sporadic FTD neurons (Figure 4B). This finding suggests that progranulin deficiency affects kinase pathways involved in cell survival, causing them to be more susceptible to inhibition of such pathways.

To validate the findings of the cell viability assay, we also measured the activation of caspase-3, a well-studied mediator of apoptotic cell death. Consistent with the results of the cell viability assay, PGRN S116X neurons showed greater caspase-3 activation in response to staurosporine than control or sporadic FTD neurons, while tunicamycin increased caspase-3 activity in both PGRN S116X and sporadic FTD neurons (Figure 4D). Because TDP-43 pathology is a hallmark in the brains of FTD patients with progranulin deficiency (Neumann et al., 2006) and increased caspase-3 activity leads to enhanced cleavage and mislocalization of TDP-43 (Zhang et al., 2007), we also analyzed the cellular distribution of TDP-43 under stress to confirm our initial findings. After exposure to staurosporine, the percentage of neurons with redistribution of TDP-43 from the nucleus to the cytoplasm was

significantly higher in PGRN S116X neurons than in control or sporadic FTD neurons (Figure S4D). In contrast, tunicamycin resulted in similar increases in the percentages of PGRN S116X and sporadic neurons with cytoplasmic TDP-43. Interestingly, in the absence of a stress inducer, the percentage of PGRN S116X neurons with cytoplasmic TDP-43 was higher than in control or sporadic FTD neurons (Figure S4D). Thus, both caspase-3 and TDP-43 assays confirm the intrinsic vulnerability of PGRN S116X neurons under stress.

Because staurosporine is a broad-spectrum kinase inhibitor that affects several signaling pathways, we next tested more specific kinase inhibitors to identify specific pathways affected by reduced progranulin levels. PGRN S116X neurons were more susceptible than control or sporadic FTD neurons to wortmannin (Figure 4C) and LY294002 (data not shown), two PI3K inhibitors, and PD98059, an MEK inhibitor (Figure S4E). These findings suggest that progranulin deficiency impairs the PI3K/Akt and MEK/MAPK signaling pathways in human neurons.

### Cellular and Molecular Defects of PGRN S116X Neurons Can be Rescued by Progranulin Expression

We next examined the causal relationship between progranulin haploinsufficiency and enhanced sensitivity to cellular stress induced by inhibitors of the PI3K/Akt and MEK/MAPK pathways in PGRN S116X neurons. To this end, we used a CS-CW-GRN-IG lentiviral vector to express progranulin in most if not all human neurons in culture. The decreased cell viability (Figure 4E) in staurosporine-treated PGRN S116X neurons was rescued by progranulin expression. A similar result was obtained when increased caspase-3 activation was used as the assay (Figure 4F), confirming the validity of the cell viability assay. In contrast, the increased sensitivity of PGRN S116X neurons to the ER stress induced by tunicamycin was not rescued by progranulin expression (Figure 4E). More importantly, the increased sensitivity of PGRN S116X neurons to inhibitors of the PI3K/Akt and MEK/MAPK pathways was also rescued (Figure 4E). Thus, the novel cellular defects of PGRN S116X neurons uncovered under stress are specific to progranulin deficiency.

Next, we sought to identify misregulated components in the PI3K/Akt and MEK/MAPK pathways by performing gene expression analysis on 2-3 replicate neuron cultures differentiated from each iPSC line and four iPSC lines per individual (30 samples total). We compared PGRN S116X neurons and sporadic FTD neurons versus control neurons, and identified a number of differentially expressed genes, both shared between PGRN S116X and sporadic FTD neurons, as well as PGRN S116X neurons-specific (Figure 4G). In addition, clustering analysis showed that gene expression patterns in neurons differentiated from three separate iPSC lines of the same individual were remarkably similar to each other (Figure 4G).

Among the top downregulated genes in PGRN S116X neurons but not in control or sporadic FTD neurons was the ribosomal protein S6 kinase beta-2 (*RPS6KB2*, Figure 4H). This gene encodes S6K2, a member of the S6 kinase family of serine/threonine kinases that has been shown to play an important role in both the PI3K/Akt and MEK/MAPK signaling pathways (Fenton and Gout, 2011), and is part of a coordinated network of differentially expressed genes including *GRN* (Figure S4H). The downregulation of the *RPS6KB2* gene was confirmed by qRT-PCR (Figure S4F) and its mRNA could be restored to wildtype level by progranulin expression (Figure S4G). More importantly, S6K2 protein level is reduced by about 50% in PGRN S116X neurons, which can be rescued to wildtype level by progranulin expression (Figure 4I, J). Taken together, these studies reveal novel cellular and molecular defects of PGRN S116X neurons in the PI3K/Akt and MEK/MAPK signaling pathways, which can be rescued by progranulin expression (Figure S4I).

## DISCUSSION

Progranulin haploinsufficiency is a major cause in FTD pathogenesis (Baker et al., 2006; Cruts et al., 2006). The underlying mechanism remains poorly understood in part due to the lack of suitable model systems. Even in *Grn* knockout mice, neuronal cell loss is limited and mechanistic studies are further complicated by the finding that progranulin levels may vary widely in patient brains in the later stages of disease (Chen-Plotkin et al., 2010). The first iPSC-based human neuronal model of progranulin haploinsufficiency established in this report provides a platform for testing small molecules that can restore progranulin levels. It also serves as a valuable and more physiologically relevant model to better understand the disease mechanisms.

FTD is an age-dependent neurodegenerative disease, some intrinsic vulnerabilities of human neurons are more likely to manifest under stress conditions in culture. Indeed, this approach has been used recently to recapitulate some key features of major neurodegenerative diseases in human neurons derived from patient-specific iPSCs (e.g. Nguyen et al., 2011). However, in contrast to well-studied Alzheimer's disease (AD) and Parkinson's disease (PD), little is known about neuronal defects in FTD patients that are caused by progranulin deficiency. Differential sensitivity of neurons to a particular stressor in culture within a short time window may reveal partially defective molecular pathways relevant to FTD pathogenesis.

Importantly, our data show that PGRN S116X neurons are more prone to reduced cell viability induced by specific protein kinase inhibitors, implicating the PI3K/Akt and MEK/MAPK signaling pathways in the molecular pathogenesis of FTD. This cellular defect is rescued by ectopic expression of progranulin in human PGRN S116X neurons, consistent with previous findings that progranulin promotes the survival of rodent primary neurons (Van Damme et al., 2008; Ryan et al., 2009; Xu et al., 2011) and that it activates the PI3K/Akt/S6K pathway in cancer cells (Zanocco-Marani et al., 1999). We also found that S6K2, a component in both PI3K/Akt and MEK/MAPK signaling pathways, is specifically downregulated in PGRN S116X neurons as part of a coordinated gene network, and its expression level can be restored to normal by ectopic progranulin expression. Interestingly, our re-analysis of the gene expression data published by Chen-Plotkin et al. (2008) revealed that *RPS6KB2* mRNA is downregulated by about 40% in the frontal cortex, but not in the hippocampus or cerebellum, of FTD patients with progranulin mutations. Taken together, these findings reinforce the notion that the PI3K/Akt and MEK/MAPK signaling pathways are compromised in PGRN S116X neurons and highlight the primary role PGRN plays in promoting neuronal survival.

ER stress and mitochondrial impairment have both been closely linked to neurodegenerative diseases (Matus et al., 2011; Schon and Przedborski, 2011). Our finding that neither PGRN S116X nor sporadic FTD neurons show enhanced sensitivity to mitochondrial or oxidative stressors argues that these pathways are unlikely to be affected by reduced progranulin levels in cultured neurons. However, mitochondrial dysfunction and oxidative stress may develop at late stages of disease progression in FTD patients.

On the other hand, both PGRN S116X and sporadic FTD neurons are more susceptible to inducers of ER stress and inhibitors of proteasome function than control neurons. This cellular defect appears to be progranulin-independent since progranulin expression levels are normal in sporadic FTD neurons. In accordance with our findings, it was recently reported that ER stress and UPR activation contribute to both sporadic FTD and familial FTD caused by *MAPT* mutations (Nijholt et al., 2012). Moreover, both A $\beta$  and increased levels of phosphorylated tau induce ER stress in AD (e.g. Hoozemans et al., 2009), as does the



accumulation of misfolded  $\alpha$ -synuclein in PD (Colla et al., 2012). Therefore, altered ER stress responses are likely to be a general feature in a variety of neurodegenerative diseases.

In summary, we establish new neuronal models of human PGRN deficiency and demonstrate specific and reversible defects affecting survival of these neurons. Our findings suggest that chronic weakening of pro-survival signaling pathways may render neurons more sensitive to environmental insults in FTD patients with progranulin deficiency. Thus, in addition to strategies to increase PGRN levels, therapeutic approaches that generally enhance neuronal survival through growth factor signaling may be beneficial in slowing disease progression in these patients.

## EXPERIMENTAL PROCEDURES

### Isolation of Primary Human Skin Fibroblasts and Generation of iPSCs

The study was approved by the Institutional Review Board and Ethics Committees at the University of California, San Francisco (UCSF), and written informed consent was obtained in all cases. The patient with the PGRN S116X mutation followed the classic clinical progression for FTD and developed parkinsonism, as all FTD patients with progranulin mutations do, but he did not show typical features of Parkinson's disease dementia. The patient with sporadic FTD also showed parkinsonism. Skin biopsies were collected, cut into small pieces, and placed on culture dishes to allow fibroblasts to expand. The cells were maintained in Dulbecco's modified Eagle's medium supplemented with 10% fetal bovine serum, 1X nonessential amino acids, and penicillin/streptomycin (100 U/mL). iPSCs were generated as described by Yamanaka and colleagues (Takahashi et al., 2007). Please see Supplementary Materials for more details.

### qRT-PCR, Immunocytochemistry, Differentiation and Characterization of iPSCs, Electrophysiology

Most of these experiments were performed as described (Delaloy et al., 2010) with minor adjustments. Please see Supplementary Materials for more details.

### PGRN Measurements

24 hours before collection, fresh culture medium was added to the cells. After the medium was collected, cells were washed once with PBS, lysed with NP-40 buffer and subjected to three freeze-thaw cycles. Both the culture medium and the cell lysates were centrifuged at 12,000 rpm at 4 °C for 10 min to clear cellular debris. Cell lysate supernatants were assayed for protein concentration with the BioRad reagent assay. Total cell lysates and culture medium were diluted, and the progranulin levels were determined with an ELISA kit (Alexis Biochemicals, San Diego, CA) according to the manufacturer's instructions. Data were normalized to protein concentration.

### Stress-induced Toxicity Assay

Two-week-old neurons were exposed to the following stress inducers for 24 h: tunicamycin, thapsigargin, rotenone, oligomycin, staurosporine, wortmannin, LY294002, PD98059, or DMSO. Cell viability was determined with the WST1 cell-proliferation assay (Roche Applied Science, Penzberg, Germany), according to the manufacturer's instructions. Caspase-3 activity assay is described in the Supplementary Materials.

### PGRN Rescue Experiments

Human *GRN* (NM\_002087.2) was inserted in a CS-CGW lentiviral vector with Nhe I and Xho I. The vector also expressed GFP through an internal ribosome entry site. One-week-

old neurons were transduced overnight with lentivirus expressing PGRN or empty vector. The next morning, the medium was doubled and thereafter replaced every other day. One week after transduction, neurons were exposed to 10 nM staurosporine, 0.5  $\mu$ M tunicamycin, 50  $\mu$ M PD98059, 75 nM wortmannin or DMSO for 24 h. Cells were assayed for cell viability, caspase-3 activation and S6K2 levels. A multiplicity of infection of 50 was used in all cases.

## Supplementary Material

Refer to Web version on PubMed Central for supplementary material.

## Acknowledgments

We thank the families of patients whose generosity made this research possible. We also thank S. Ordway for editorial assistance, J.A. Lee for help at the early stage of this project, and J. Miller and Gao lab members for discussions. This work was initiated with a grant from the California Institute for Regenerative Medicine (RL1-00650, FBG and RVF Jr.) and supported by startup funds from the University of Massachusetts Medical School (FBG and KF). This work was also partially supported by the National Institutes of Health (NS057553, FBG; AG019724 and AG023501, BLM), the Consortium for FTD Research (FBG and DHG).

## REFERENCES

- Ahmed Z, Sheng H, Xu YF, Lin WL, Innes AE, Gass J, Yu X, Wuertzer CA, Hou H, Chiba S, et al. Accelerated lipofuscinosis and ubiquitination in granulin knockout mice suggest a role for progranulin in successful aging. *Am. J. Pathol.* 2010; 177:311–324. [PubMed: 20522652]
- Baker M, Mackenzie IR, Pickering-Brown SM, Gass J, Rademakers R, Lindholm C, Snowden J, Adamson J, Sadovnick AD, Rollinson S, et al. Mutations in progranulin cause tau-negative frontotemporal dementia linked to chromosome 17. *Nature.* 2006; 442:916–919. [PubMed: 16862116]
- Boxer AL, Miller BL. Clinical features of frontotemporal dementia. *Alzheimer Dis. Assoc. Disord.* 2005; 19(Suppl 1):S3–6. [PubMed: 16317256]
- Chen-Plotkin AS, Xiao J, Geser F, Martinez-Lage M, Grossman M, Unger T, Wood EM, Van Deerlin VM, Trojanowski JQ, Lee VM. Brain progranulin expression in GRN-associated frontotemporal lobar degeneration. *Acta Neuropathol.* 2010; 119:111–122. [PubMed: 19649643]
- Chen-Plotkin AS, Geser F, Plotkin JB, Clark CM, Kwong LK, Yuan W, Grossman M, Van Deerlin VM, Trojanowski JQ, Lee VM. Variations in the progranulin gene affect global gene expression in frontotemporal lobar degeneration. *Hum. Mol. Genet.* 2008; 17:1349–1362. [PubMed: 18223198]
- Colla E, Coune P, Liu Y, Pletnikova O, Troncoso JC, Iwatsubo T, Schneider BL, Lee MK. Endoplasmic reticulum stress is important for the manifestations of  $\alpha$ -synucleinopathy in vivo. *J. Neurosci.* 2012; 32:3306–3320. [PubMed: 22399753]
- Coppola G, Kadas A, Rademakers R, Wang Q, Baker M, Hutton M, Miller BL, Geschwind DH. Gene expression study on peripheral blood identifies progranulin mutations. *Ann. Neurol.* 2008; 64:92–96. [PubMed: 18551524]
- Cruts M, Gijselink I, van der Zee J, Engelborghs S, Wils H, Pirici D, Rademakers R, Vandenberghe R, Dermaut B, J J, Martin JJ, et al. Null mutations in progranulin cause ubiquitin-positive frontotemporal dementia linked to chromosome 17q21. *Nature.* 2006; 442:920–924. [PubMed: 16862115]
- DeJesus-Hernandez M, Mackenzie IR, Boeve BF, Boxer AL, Baker M, Rutherford NJ, Nicholson AM, Finch NA, Flynn H, Adamson J, et al. Expanded GGGGCC hexanucleotide repeat in noncoding region of C9ORF72 causes chromosome 9p-linked FTD and ALS. *Neuron.* 2011; 72:245–256. [PubMed: 21944778]
- Delalay C, Liu L, Lee J-A, Su H, Shen F, Yang GY, Young WL, Ivey KN, Gao FB. MicroRNA-9 coordinates proliferation and migration of human embryonic stem cells-derived neural progenitors. *Cell Stem Cell.* 2010; 6:323–335. [PubMed: 20362537]

- Dimos JT, Rodolfa KT, Niakan KK, Weisenthal LM, Mitsumoto H, Chung W, Croft GF, Saphier G, Leibel R, Golland R, et al. Induced pluripotent stem cells generated from patients with ALS can be differentiated into motor neurons. *Science*. 2008; 321:1218–1221. [PubMed: 18669821]
- Ebert AD, Yu J, Rose FF Jr, Mattis VB, Lorson CL, Thomson JA, Svendsen CN. Induced pluripotent stem cells from a spinal muscular atrophy patient. *Nature*. 2009; 457:277–280. [PubMed: 19098894]
- Fenton TR, Gout IT. Functions and regulation of the 70kDa ribosomal S6 kinases. *Int. J. Biochem. Cell Biol.* 2011; 43:47–59. [PubMed: 20932932]
- Freberg CT, Dahl JA, Timoskainen S, Collas P. Epigenetic reprogramming of OCT4 and NANOG regulatory regions by embryonal carcinoma cell extract. *Mol. Biol. Cell*. 2007; 18:1543–1553. [PubMed: 17314394]
- Finch N, Baker M, Crook R, Swanson K, Kuntz K, Surtees R, Bisceglia G, Rovelet-Lecrux A, Boeve B, Petersen RC, et al. Plasma progranulin levels predict progranulin mutation status in frontotemporal dementia patients and asymptomatic family members. *Brain*. 2010; 132:583–591. [PubMed: 19158106]
- Ghoshal N, Dearborn JT, Wozniak DF, Cairns NJ. Core features of frontotemporal dementia recapitulated in progranulin knockout mice. *Neurobiol. Dis.* 2012; 45:395–408. [PubMed: 21933710]
- He Z, A. Bateman A. Progranulin (granulin-epithelin precursor, PC cell-derived growth factor, acrogranin) mediates tissue repair and tumorigenesis. *J. Mol. Med.* 2003; 81:600–612. [PubMed: 12928786]
- Hoozemans JJ, van Haastert ES, Nijholt DA, Rozemuller AJ, Eikelenboom P, Scheper W. The unfolded protein response is activated in pretangle neurons in Alzheimer's disease hippocampus. *Am. J. Pathol.* 2009; 174:1241–1251. [PubMed: 19264902]
- Israel MA, Yuan SH, Bardy C, Reyna SM, Mu Y, Herrera C, Hefferan MP, Gorp SP, Nazor KL, Boscolo FS, Carson CT, et al. Probing sporadic and familial Alzheimer's disease using induced pluripotent stem cells. *Nature*. 2012; 482:216–220. [PubMed: 22278060]
- Matus S, Glimcher LH, Hetz C. Protein folding stress in neurodegenerative diseases: a glimpse into the ER. *Curr. Opin. Cell Biol.* 2011; 23:239–252. [PubMed: 21288706]
- Napoli I, Kierdorf K, Neumann H. Microglial precursors derived from mouse embryonic stem cells. *Glia*. 2009; 57:1660–1671. [PubMed: 19455585]
- Neumann M, Sampathu DM, Kwong LK, Truax AC, Micsenyi MC, et al. Ubiquitinated TDP-43 in frontotemporal lobar degeneration and amyotrophic lateral sclerosis. *Science*. 2006; 314:130–133. [PubMed: 17023659]
- Nguyen HN, Byers B, Cord B, Shcheglovitov A, Byrne J, Gujar P, Kee K, Schüle B, Dolmetsch RE, et al. LRRK2 mutant iPSC-derived DA neurons demonstrate increased susceptibility to oxidative stress. *Cell Stem Cell*. 2011; 8:267–280. [PubMed: 21362567]
- Nijholt DA, van Haastert ES, Rozemuller AJ, Scheper W, Hoozemans JJ. The unfolded protein response is associated with early tau pathology in the hippocampus of tauopathies. *J. Pathol.* 2012; 226:693–702. [PubMed: 22102449]
- Petkau TL, Neal SJ, Milnerwood A, Mew A, Hill AM, Orban P, Gregg J, Lu G, Feldman HH, et al. Synaptic dysfunction in progranulin-deficient mice. *Neurobiol. Dis.* 2012; 45:711–722. [PubMed: 22062772]
- Ryan CL, Baranowski DC, Chitramuthu BP, Malik S, Li Z, Cao M, Minotti S, Durham HD, Kay DG, Shaw CA, et al. Progranulin is expressed within motor neurons and promotes neuronal cell survival. *BMC Neurosci.* 2009; 10:130. [PubMed: 19860916]
- Renton AE, Majounie E, Waite A, Simón-Sánchez J, Rollinson S, Gibbs JR, Schymick JC, Laaksovirta H, van Swieten JC, Myllykangas L, et al. A hexanucleotide repeat expansion in C9ORF72 is the cause of chromosome 9p21-linked ALS-FTD. *Neuron*. 2011; 72:257–268. [PubMed: 21944779]
- Schon EA, Przedborski S. Mitochondria: the next (neurode)generation. *Neuron*. 2011; 70:1033–1053. [PubMed: 21689593]

- Skibinski G, Parkinson NJ, Brown JM, Chakrabarti L, Lloyd SL, Hummerich H, Nielsen JE, Hodges JR, Spillantini MG, Thusgaard T, et al. Mutations in the endosomal ESCRTIII-complex subunit CHMP2B in frontotemporal dementia. *Nat. Genet.* 2005; 37:806–808. [PubMed: 16041373]
- Soldner F, Hockemeyer D, Beard C, Gao Q, Bell GW, Cook EG, Hargus G, Blak A, Cooper O, Mitalipova M, Isacson O, Jaenisch R. Parkinson's disease patient-derived induced pluripotent stem cells free of viral reprogramming factors. *Cell.* 2009; 136:964–977. [PubMed: 19269371]
- Tapia L, Milnerwood A, Guo A, Mills F, Yoshida E, Vasuta C, Mackenzie IR, Raymond L, Cynader M, Jia W, Bamji SX. Progranulin deficiency decreases gross neural connectivity but enhances transmission at individual synapses. *J. Neurosci.* 2011; 31:11126–11132. [PubMed: 21813674]
- Takahashi K, Tanabe K, Ohnuki M, Narita M, Ichisaka T, Tomoda K, Yamanaka S. Induction of pluripotent stem cells from adult human fibroblasts by defined factors. *Cell.* 2007; 131:861–872. [PubMed: 18035408]
- Van Damme P, Van Hoecke A, Lambrechts D, Vanacker P, Bogaert E, van Swieten J, Carmeliet P, Van Den Bosch L, Robberecht W. Progranulin functions as a neurotrophic factor to regulate neurite outgrowth and enhance neuronal survival. *J. Cell. Biol.* 2008; 181:37–41. [PubMed: 18378771]
- Watts GD, Wymer J, Kovach MJ, Mehta SG, Mumm S, Darvish D, Pestronk A, Whyte MP, Kimonis VE. Inclusion body myopathy associated with Paget disease of bone and frontotemporal dementia is caused by mutant valosin-containing protein. *Nat. Genet.* 2004; 36:377–381. [PubMed: 15034582]
- Xu J, Xilouri M, Bruban J, Shioi J, Shao Z, Papazoglou I, Vekrellis K, Robakis NK. Extracellular progranulin protects cortical neurons from toxic insults by activating survival signaling. *Neurobiol. Aging.* 2011; 32:2326.e5–16. [PubMed: 21820214]
- Yamanaka S. Strategies and new developments in the generation of patient-specific pluripotent stem cells. *Cell Stem Cell.* 2007; 1:39–49. [PubMed: 18371333]
- Yin F, Banerjee R, Thomas B, Zhou P, Qian L, Jia T, Ma X, Ma Y, Iadecola C, Beal MF, et al. Exaggerated inflammation, impaired host defense, and neuropathology in progranulin-deficient mice. *J. Exp. Med.* 2010; 207:117–128. [PubMed: 20026663]
- Zanocco-Marani T, Bateman A, Romano G, Valentinis B, He ZH, Baserga R. Biological activities and signaling pathways of the granulin/epithelin precursor. *Cancer Res.* 1999; 59:5331–5340. [PubMed: 10537317]
- Zhang YJ, Xu YF, Dickey CA, Buratti E, Baralle F, Bailey R, Pickering-Brown S, Dickson D, Petrucelli L. Progranulin mediates caspase-dependent cleavage of TAR DNA binding protein-43. *J. Neurosci.* 2007; 27:10530–10534. [PubMed: 17898224]

**HIGHLIGHTS**

- Multiple iPSC lines were made from sporadic and progranulin-deficient FTD patients.
- A human neuron model of progranulin haploinsufficiency has been established.
- PGRN S116X neurons are more sensitive to stress induced by several kinase inhibitors.
- S6K2 is downregulated in patient neurons in a progranulin-dependent manner.

\$watermark-text

\$watermark-text

\$watermark-text

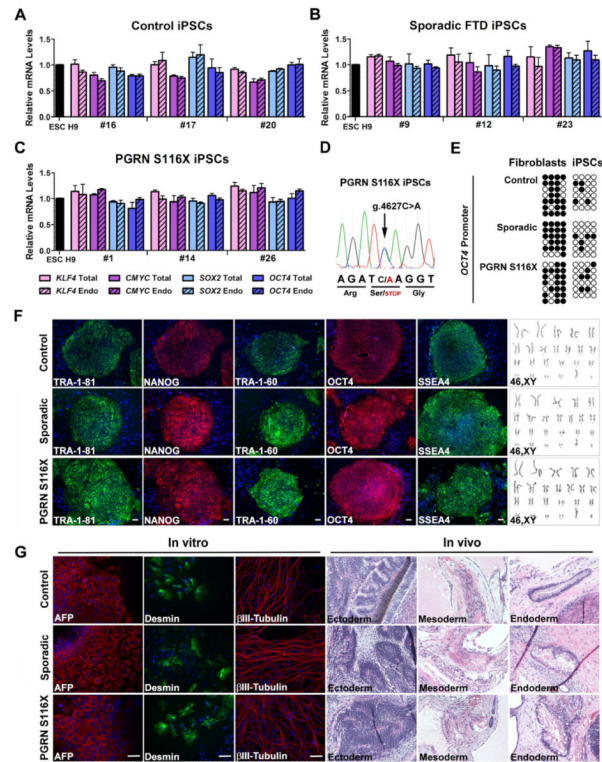


### Figure 1. Generation and Characterization of FTD Patient-Specific iPSCs

(A-C) Total and endogenous (Endo) levels of the reprogramming factors in control, sporadic, and PGRN S116X iPSC lines relative to the values in H9, as assessed by qRT-PCR. Values are mean  $\pm$  SEM.

(D) Genomic DNA sequencing of the heterozygous PGRN S116X mutation g.4627C>A (p.S116X: nonsense mutation) in PGRN S116X iPSCs.

(E) Methylation status of the *OCT4* promoter for control iPSC line 20, sporadic iPSC line 9, and PGRN S116X iPSC line 26. Open circles, unmethylated CpG dinucleotides. Filled circles, methylated CpG dinucleotides.

(F) Immunofluorescence analysis of pluripotency markers in control iPSC line 20, sporadic iPSC line 9, and PGRN S116X iPSC line 26, and their respective normal karyotypes. Cell nuclei were counterstained with DAPI (blue). Scale bar, 50  $\mu$ m.

(G) In vitro (EB formation) and in vivo (teratoma formation) differentiation of control iPSC line 20, sporadic iPSC line 9, and PGRN S116X iPSC line 26 into cells of all three germ layers. For in vitro studies, cells were immunostained with  $\alpha$ -fetoprotein (AFP, endoderm), desmin (mesoderm),  $\beta$ III-tubulin (ectoderm), and DAPI (nuclei). Hematoxylin/eosin staining of teratoma sections showed neuron/rosette structures (ectoderm), smooth muscle (mesoderm), and ducts (endoderm). Scale bar, 50  $\mu$ m.

See also Figure S1.

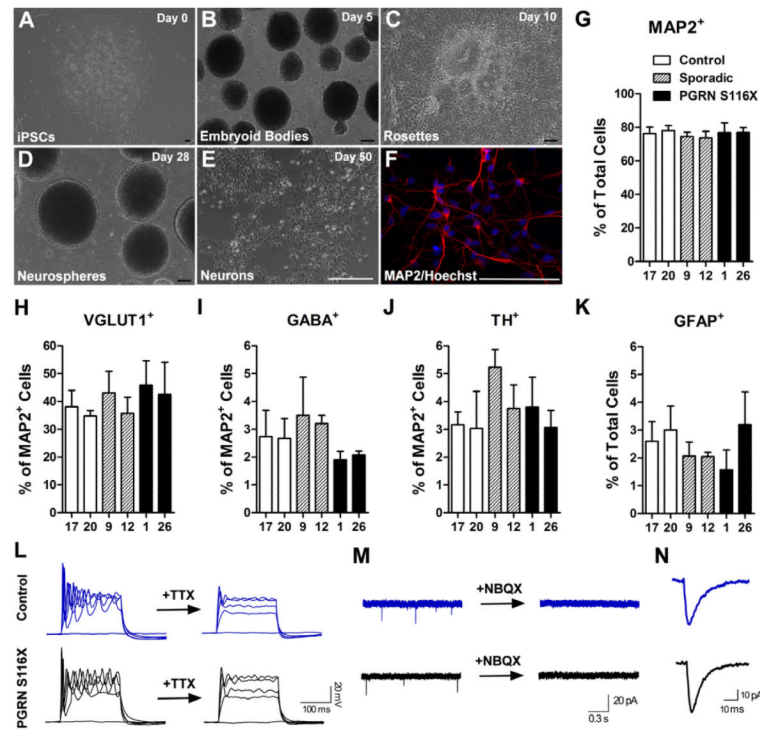


**Figure 2. Differentiation and Characterization of Human Postmitotic Neurons Derived from FTD and Control iPSCs**

(A-E) Phase-contrast images of the cells at different stages of neuronal differentiation. Scale bar, 100  $\mu$ m.

(F) Representative images of 2-week-old cells stained with MAP2. Nuclear staining is shown in blue.

(G, K) Cells positive for MAP2 and GFAP as a percentage of all cells in 2-week-old cultures.

(H-J) Cells positive for VGLUT1, GABA, and TH (glutamatergic, GABAergic and dopaminergic markers, respectively) as a percentage of MAP<sup>+</sup> cells. On average, 200 cells were analyzed per experiment in panels G-K ( $n = 3$  independent cultures). Values are mean  $\pm$  SEM. (L) Electrophysiological properties of control neurons and PGRN S116X neurons. Representative action potentials responding to step depolarization by current injection from 0 pA to 400 pA (100 pA step) that could be blocked by tetrodotoxin.  $n = 24$  for each line.

(M) Sample traces of mEPSCs from control (blue) and PGRN S116X neurons (black). All neurons ( $n = 10$  for each line) displayed synaptic responses and were abolished by AMPA receptor antagonist NBQX.

(N) Averaged mEPSC traces from control (blue) and PGRN S116X neurons (black).

See also Figure S2.

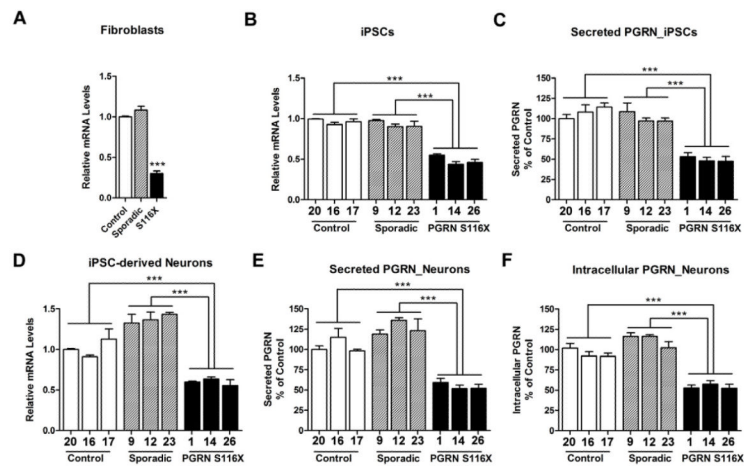


**Figure 3. An FTD Patient-Specific Neuronal Model of Progranulin Haploinsufficiency**

(A) *GRN* mRNA expression levels in fibroblasts.

(B, D) *GRN* mRNA expression levels in iPSC lines derived from control, sporadic, and PGRN S116X subjects (B) and neurons differentiated from iPSCs (D). The values from control (fibroblasts) or control line 20 were set to 1 (n = 3-4 independent cultures).

(C, E) Amount of progranulin secreted into the medium over 24 h by iPSCs (C) and iPSC-derived neurons (E). Values of control line 20 were set to 100% (n = 3-4 independent cultures).

(F) Intracellular progranulin levels in iPSC-derived neurons after medium collection. Values of control line 20 were set to 100% (n = 3-4 independent cultures). In panels (A-F), Values are mean  $\pm$  SEM. \*\* $p < 0.01$ ; \*\*\* $p < 0.001$ , patient cells were compared with control cells. See also Figure S3.



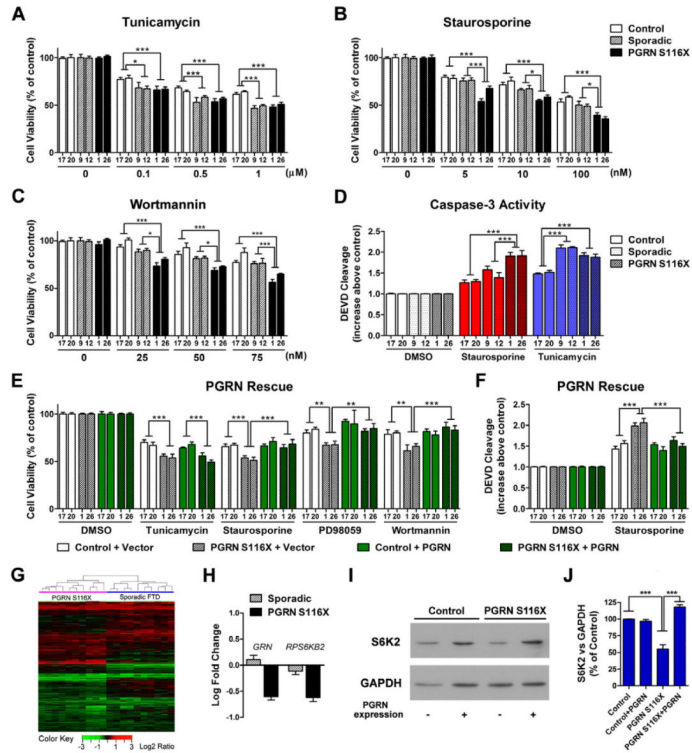


#### Figure 4. Novel Cellular and Molecular Defects of PGRN S116X Neurons Can be Rescued by Progranulin Expression

(A-C) Effects of the stress inducers on human neurons. Values are expressed as a percentage of the cells exposed to DMSO (control) ( $n = 3-4$  independent cultures).

(D) Caspase-3-like activity after exposure to 10 nM staurosporine, 0.5  $\mu$ M tunicamycin, or DMSO for 24 h.

(E and F) Measurement of cell viability (E) and caspase-3 activation (F) after rescue with progranulin expression.  $n=5-6$  independent cultures.

(G) Heatmap depicting fold changes of gene expression in 2-3 neuron cultures differentiated from each one of the four iPSC lines of sporadic FTD case (blue) or PGRN S116X patient (fuchsia) compared to control neurons.

(H) Gene expression changes on the array for *GRN* and *RPS6KB2*. The log fold change is relative to control neurons.

(I and J) Progranulin expression restores S6K2 protein levels in PGRN S116X neurons.

Representative western blotting image for S6K2 (control line 17 and PGRN S116X line 1)

(I) and quantification of S6K2 relative to GAPDH for three experiments performed on lines 17 and 20 (control) and, 1 and 26 (PGRN S116X) (J). In all panels, values are mean  $\pm$  SEM.

\*:  $p < 0.05$ , \*\*:  $p < 0.01$ , \*\*\*:  $p < 0.001$ .

See also Figure S4.